

MMANOVA: A general multilevel framework for multivariate analysis of variance

Steven Geinitz

geinitz@math.uzh.ch

University of Zurich

Reinhard Furrer

furrer@math.uzh.ch

University of Zurich

Stephan R. Sain

ssain@ucar.edu

National Center for
Atmospheric Research

1 **Abstract** Classical analysis of variance requires that model terms be labeled as
2 fixed or random and typically culminate by comparing variability from each batch
3 (factor) to variability from errors; without a standard methodology to assess the
4 magnitude of a batch's variability, to compare variability between batches, nor to
5 consider the uncertainty in this assessment. In this paper we support recent work,
6 placing ANOVA into a general multilevel framework, then refine this through batch
7 level model specifications, and develop it further by extension to the multivari-
8 ate case. Adopting a Bayesian multilevel model parametrization, with improper
9 batch level prior densities, we derive a method that facilitates comparison across
10 all sources of variability. Whereas classical multivariate ANOVA often utilizes a
11 single covariance criterion, e.g. determinant for Wilks' lambda distribution, the
12 method allows arbitrary covariance criteria to be employed. The proposed method
13 also addresses computation. By introducing implicit batch level constraints, which
14 yield improper priors, the full posterior is efficiently factored, thus alleviating com-
15 putational demands. For a large class of models, the partitioning mitigates, or
16 even obviates the need for methods such as MCMC. The method is illustrated with
17 simulated examples and an application focusing on climate projections with global
18 climate models.

19
20 *Keywords:* Bayesian inference; Constraints; Mixed model; Variance components

1 Introduction

Identifying and comparing variability among several factors is a fundamental task of statistical analysis. From initial exploratory steps, to model testing, analysis of variance plays a vital role in the practice of statistics. Gelman (2005) has outlined a general ANOVA methodology that fits a wide range of models and summarizes results in a manner that facilitates interpretation across different sources of variation. Gelman and Hill (2006) elaborate further, describing the methodology in terms of a multilevel model. One important contribution of this approach is in providing summaries that are more constructive than conclusions based on hypothesis tests. This framework is seeing usage by researchers from diverse fields e.g. ecology (Qian and Shen, 2007), genetics (Leinonen *et al.*, 2008), and climate (Sain *et al.*, 2011).

This paper presents a method that adopts the multilevel approach towards ANOVA, then extends it to multivariate settings, yielding a multilevel multivariate analysis of variance (MMANOVA) methodology. The strategy of initially treating all sources of variability in similar regard is naturally a part of the new method. We address known issues of applying constraints in variance analyses (Nelder, 1977, 1994, 1999) by constraining batch levels so that prior distributions are improper. The extension is seen as a valuable contribution, since multivariate ANOVA can further obfuscate model specification, interpretation, and computation. Kaufman and Sain (2010) offer an analysis of variance procedure that aids in model specification and interpretation, but requires computationally demanding MCMC steps. Recent methods involving approximations, e.g. integrated nested Laplace approximations (INLA) (Lindgren *et al.*, 2011; Rue *et al.*, 2009), have allowed for MCMC to be eliminated in many cases, significantly reducing computational demands. While the range of problems for which such methods are applicable is wide, the focus is not typically on variance parameters. Thus, the contribution of our work is in promoting a general ANOVA methodology. We accomplish this by supporting recent work with the same goal, by refining the model specification, and by extending this to multivariate cases.

49 In Section 2 we review the ANOVA formulation of Gelman (2005) and summarize
50 some details of the approach. We then formally extend the idea to the multivariate
51 case, discussing technical and computational aspects. Section 3 provides a demonstration
52 of the method through a simulation example and through a climatological application
53 using data from future climate projections given by several atmosphere-ocean general
54 circulation models and global emissions scenarios. In Section 4 we discuss extensions and
55 further computational benefits that are possible when the method is applied to common
56 high-dimensional problems.

57 **2 Analysis of Variance**

58 Analysis of variance is widely accepted as a means of partitioning variability in a manner
59 which allows it to be attributed to various factors. An important initial step in the
60 analysis is considering each factor of the model to be fixed or random. This step, necessary
61 in the classical setting, raises enough issues that statisticians have been obliged to address
62 the “mixed models controversy” (Lencina *et al.*, 2005; Voss, 1999). One might conclude
63 that a consensus has still not been reached, given that John Nelder deemed it necessary
64 to reiterate the requisite points of constraints and marginality over such a long period of
65 time, beginning with Nelder (1977) and most recently Nelder (2008).

66 The rest of the section outlines a recent attempt by Gelman (2005) towards a more
67 universal ANOVA methodology, then refines and extends the approach to a multivariate
68 context.

69 **2.1 Multilevel ANOVA**

70 A fundamental contribution of the hierarchical regression approach to ANOVA employed
71 by Gelman (2005) has been to indiscriminately consider all components in a model as
72 random, thereby facilitating comparison across all sources of variability. The terminology
73 is useful in supporting the indiscriminate nature of the method. The word *batch* is
74 applied to all terms in the model, e.g. overall mean, factors, nested terms, interactions,

75 etc. The nature of the variability from a batch is further distinguished. The distinction
 76 traditionally made by random and fixed effects is instead addressed by considering a
 77 batch's *super* and *finite* population variance. We now summarize the recent shift in
 78 ANOVA as a methodology in terms of a univariate linear model.

79 2.1.1 Model Parametrization

80 Following the notation of Gelman (2005), observations $Y_i, i = 1, \dots, n$ are stated in terms
 81 of the additive decomposition

$$Y_i = \sum_{b=0}^B \beta_{j_i^b}^{(b)}, \quad (1)$$

82 or the alternative regression formulation

$$Y_i = \sum_{b=0}^B \sum_{j=1}^{n_B} x_{i,j}^{(b)} \beta_{j^b}^{(b)}, \quad (2)$$

83 with $\beta_{j^b}^{(b)}$ denoting individual batch levels and $x_{i,j}$ denoting explanatory variables. The
 84 regression formulation could be used for the additive decomposition, with explanatory
 85 variables set to either 0 or 1. Batch indices $b = 0$ and $b = B$ will often correspond to an
 86 overall mean, μ , and to measurement errors, ϵ_i , respectively, so that $n_0 = 1, n_B = n$. An
 87 individual batch is referenced by $b = 0, \dots, B$ and consists of n_b levels. Individual levels
 88 of a batch are denoted as $\beta_1^{(b)}, \dots, \beta_{n_b}^{(b)}$ with $j_1^b, \dots, j_{n_b}^b$ replicating the levels so that each
 89 observation is associated with exactly one batch level. We acknowledge that the additional
 90 level of subscripts and superscripts may seem contrived to some, although it is necessary
 91 for the general case. In practice the number of batches in the model is reasonable so
 92 that this can be avoided, as done in Section 3. Additional sub or superscripts can often
 93 be dropped. For example, a batch in its entirety is denoted by $\beta^{(b)} = \{\beta_1^{(b)}, \dots, \beta_{n_b}^{(b)}\}$.
 94 Given a batch, and an assumed distribution on model errors, a conventional fixed effects
 95 analysis often corresponds to the test $H_0: \beta_j^{(b)} = 0$ for $j = 1, \dots, n_b$. While for a random
 96 effects model, assuming the n_b levels of each batch b to be modeled as Gaussian

$$\beta_j^{(b)} \mid \sigma_b^2 \sim N(0, \sigma_b^2), \quad j = 1, \dots, n_b, \quad (3)$$

97 a test for significant batch variation would be $H_0 : \sigma_b^2 = 0$. Alternatively, the proposed
 98 methodology identifies two representations of variation of a given batch. The superpopu-
 99 lation variance, σ_b^2 , corresponds to the variance of all potential, possibly infinitely many,
 100 levels of a batch. The finite-population variance represents variability of the specific set of
 101 batch levels that have been realized. Super and finite-population variances can be roughly
 102 related to the random effect variance component estimate, and the fixed effect within-
 103 group sum of squares, respectively. As an example, consider batch b and its vector of batch
 104 levels, $\boldsymbol{\beta}^{(b)} = (\beta_1^{(b)}, \dots, \beta_{n_b}^{(b)})^T$ with c_b constraints. Then the degrees of freedom are $\nu_b =$
 105 $n_b - c_b$, and the finite-population variance s_b^2 is $s_b^2 = \frac{1}{\nu_b} \boldsymbol{\beta}^{(b)T} (\mathbf{I}_{n_b} - \mathbf{C}_b^T (\mathbf{C}_b \mathbf{C}_b^T)^{-1} \mathbf{C}_b) \boldsymbol{\beta}^{(b)}$,
 106 where \mathbf{I}_{n_b} is the $n_b \times n_b$ identity and \mathbf{C}_b is the $c_b \times n_b$ constraint matrix such that
 107 $\mathbf{C}_b \boldsymbol{\beta}^{(b)} = \mathbf{0}$. Variance component estimation is made by decomposing the variance of the
 108 batch level estimates, $V_b = \text{Var}(\widehat{\boldsymbol{\beta}}^{(b)}) = \text{Var}\{\text{E}(\widehat{\boldsymbol{\beta}}^{(b)} \mid \boldsymbol{\beta}^{(b)})\} + \text{E}\{\text{Var}(\widehat{\boldsymbol{\beta}}^{(b)} \mid \boldsymbol{\beta}^{(b)})\}$, into the
 109 sum of the superpopulation variation, σ_b^2 , plus the variability of the batch level estima-
 110 tions, $V_{\text{b:estimation}}$. The chosen estimate of the superpopulation variance, in this case the
 111 method-of-moments estimator, is then $\widehat{\sigma}_b^2 = \widehat{V}_b - \widehat{V}_{\text{b:estimation}}$, where, $\widehat{V}_b = \frac{1}{\nu_b} \sum_{j=1}^{n_b} (\widehat{\beta}_j^{(b)})^2$,
 112 and $\widehat{V}_{\text{b:estimation}} = \sum_{k \in I(b)} \frac{n_b}{n_k} \widehat{\sigma}_k^2$ includes superpopulation variances from other batches
 113 that enter into variability of the batch level estimates, indicated by the set $I(b)$. At a
 114 minimum, $\widehat{V}_{\text{b:estimation}}$ will include $\widehat{\sigma}_B^2$, the estimated error variance. For a large class of
 115 multilevel, hierarchical models, this strategy allows for all terms to be treated as random,
 116 and for their variabilities to be assessed.

117 2.1.2 Confirmatory Procedures

118 In regards to more inferential procedures, either a frequentist or Bayesian direction can
 119 be taken. In the frequentist case, an inverse-chi-square distribution, χ_{ν}^{-2} , is employed
 120 to assess uncertainty in the superpopulation variance σ_b^2 ; since $\frac{1}{\nu_b} s_b^2 / \sigma_b^2$ is chi-square dis-
 121 tributed with ν_b degrees of freedom. For batches with $\sum_{k \in I(b)} \frac{n_b}{n_k} \widehat{\sigma}_k^2$, including more than
 122 only the error variance $\widehat{\sigma}_B^2$, then a linear combination of inverse-chi-square distributions,
 123 $\sum_i m_i \chi_{\nu_i}^{-2}$, is required, as described at the end of the previous section. As Gelman (2005)

124 states, these linear combinations may be dealt with directly, although simulation is often
125 more straightforward. The simulation, described therein, is carried out by: 1) Obtain
126 R simulated raw variances, V_b for each of the B batches in the model with a random
127 variable that is proportional to χ^{-2} and corresponding degrees of freedom; 2) Calculate
128 superpopulation variances using $\hat{\sigma}_b^2 = \max(0, V_b - V_{b:\text{estimation}})$; 3) Simulate batch levels
129 using newly generated superpopulation variances; 4) Calculate sample variances of each
130 batch. This procedure then yields a (posterior) sample of superpopulation variances,
131 batch levels, and finite-population variances, corresponding to the final three steps.

132 A strict Bayesian approach requires additional prior specifications, but yields posterior
133 distributions of the superpopulation variances. However, this distinction, between the
134 two schools of thought, can be seen as purely semantic. As Gelman (2005) states, “given
135 σ_b^2 , the parameters $\beta_j^{(b)}$ have a multivariate normal distribution (in Bayesian terms, a
136 conditional posterior distribution; in classical terms, a predictive distribution)”. Thus,
137 assessing uncertainty in the finite-population variances, s_b^2 , is the same. In both cases,
138 either batch levels themselves are simulated, or the distribution of s_b^2 is approximated
139 with an appropriate chi-square random variable.

140 It should be clear that the uncertainty surrounding superpopulation variance param-
141 eters will typically be greater than that for finite-population variances. Intuitively, this
142 is because superpopulation variances describe variability of levels that have not yet been
143 realized.

144 2.2 Multilevel Multivariate ANOVA

145 Typical multivariate analysis of variance strategies rely on the distribution of the de-
146 terminant of sums of squares matrices, i.e. Wilks’ lambda distribution (Mardia *et al.*,
147 1979, p. 335), and culminate in p -value related conclusions. Hence, it does not easily
148 facilitate inclusion of random effects, and thus no comparison across these effects. Using
149 a Bayesian approach, we now derive a general multivariate methodology that seeks to
150 provide results similar to those of Section 2.1.1. The method partitions variability by

151 batch in an efficient manner and further factors the posterior by batch into a batch's
152 superpopulation covariance posterior, and batch levels posteriors. In addition, we handle
153 the issue of constraints in a way that does not commit what Nelder (1994) has called
154 one of the false steps of linear models. Rather, the constraints are implicit, yielding im-
155 proper batch level prior distributions. Another point which must be mentioned is that
156 of matrix parameter estimation. Although the common limitations of covariance matrix
157 estimation and modeling are issues that must be dealt with, it is important to first focus
158 on, and refine multivariate ANOVA for familiar settings. In Section 4 we discuss issues,
159 modifications, and implications of the method when higher dimensional data is used.

160 2.2.1 Multivariate Model Parametrization

161 Consider d -dimensional multivariate observations such that batch levels are vectors and
162 batch variances are covariance matrices. Namely, (1)–(3) now contain vectors \mathbf{Y}_i , $\boldsymbol{\beta}_{j^b}^{(b)}$,
163 matrices $\mathbf{X}_{i,j}$, and covariance matrices are $\boldsymbol{\Sigma}_b$, all of appropriate dimension. We adopt the
164 strategy from the previous section, in indiscriminately considering all terms as potentially
165 possessing variability. The multivariate analogue of (1) with Gaussian errors is

$$\mathbf{Y}_i \mid \{\boldsymbol{\beta}_{j^b}^{(b)}\}_b, \boldsymbol{\Sigma}_\epsilon \sim \mathcal{N}_d \left(\sum_{b=0}^{B-1} \boldsymbol{\beta}_{j^b}^{(b)}, \boldsymbol{\Sigma}_\epsilon \right), \quad i = 1, \dots, n, \quad (4)$$

166 and the remainder of the Bayesian model specification is given by

$$\boldsymbol{\beta}_j^{(b)} \mid \boldsymbol{\Sigma}_b \sim \mathcal{N}_d(\boldsymbol{\beta}_0^{(b)}, \boldsymbol{\Sigma}_b), \quad j = 1, \dots, n_b, \quad (5)$$

$$\mathbf{U}_b = \boldsymbol{\Sigma}_b + \frac{n_b}{n} \boldsymbol{\Sigma}_\epsilon \mid \boldsymbol{\Sigma}_\epsilon \sim W^{-1}(\boldsymbol{\Psi}_b, \kappa_b), \quad (6)$$

$$\boldsymbol{\Sigma}_\epsilon \sim W^{-1}(\boldsymbol{\Psi}_\epsilon, \kappa_\epsilon), \quad (7)$$

167 for $b = 0, \dots, B - 1$ and with the inverse-Wishart distribution denoted by W^{-1} . Batch
168 indices $b = 0$ and $b = B$ respectively correspond to the intercept, or overall mean term,
169 $\boldsymbol{\mu}$, and to measurement errors, $\boldsymbol{\epsilon}_i$. For notational convenience we will refer to $\boldsymbol{\Sigma}_\mu$ and
170 $\boldsymbol{\Sigma}_\epsilon$, rather than $\boldsymbol{\Sigma}_0$ and $\boldsymbol{\Sigma}_B$. Typically zero-mean batch level priors are assumed; that is,
171 $\boldsymbol{\beta}_0^{(b)} = \mathbf{0}$. Setting $\boldsymbol{\Psi}_b = \mathbf{0}$, $\kappa_b = 0$ yields the noninformative prior $p(\mathbf{U}_b) \propto |\mathbf{U}_b|^{-(d+1)/2}$.

172 Because inverse-Wishart support is given by the set of all positive definite matrices, (6) is
 173 referred to as a constrained inverse-Wishart distribution, since $\mathbf{U}_b - \frac{n_b}{n}\boldsymbol{\Sigma}_\epsilon$ is required to be
 174 positive definite. This covariance parametrization, $\mathbf{U}_b = \boldsymbol{\Sigma}_b + \frac{n_b}{n}\boldsymbol{\Sigma}_\epsilon$, has previously been
 175 utilized in the context of multivariate random effects by Everson and Morris (2000), for
 176 which they develop efficient methods of sampling. Also, when only error terms contribute
 177 to the variance of batch level estimates, \mathbf{U}_b is analogous to V_b of Section 2.1.1 with
 178 $I(b) = \{B\}$.

179 The choice of inverse-Wishart covariance priors, (6) and (7), has been made to balance
 180 the complexity of model specification with implementation and computation. However,
 181 given the considerable amount of research of covariance priors, there are other options
 182 available. Daniels (1999) and Daniels and Kass (2001) examine covariance priors that
 183 emphasize uniform shrinkage of the eigenvalues. Although informative covariance priors
 184 may be necessary in many cases, the usage of such priors will impact the computational
 185 demands required.

186 2.2.2 Posterior Distributions

187 Without additional specification, (4)–(7) yield an inadequate posterior. In an MCMC
 188 setting this may manifest itself by failure to converge, due to drifting in the parameter
 189 space. From a classical point of view, estimating the set of all batch levels, $\{\boldsymbol{\beta}_{j^b}^{(b)}\}$ would
 190 require additional constraints. The inclusion of similar constraints in the Bayesian model
 191 allows for a closed form of the posterior, as well as for factorization between batches.
 192 Degrees of freedom for each batch are then accounted for in the corresponding batch
 193 covariance posterior. This parametrization is also beneficial in terms of computation
 194 since batches are conditionally independent of one another. Using a vectorized form of
 195 the model, $\mathbf{Y} = (\mathbf{Y}_1^T, \dots, \mathbf{Y}_n^T)^T \in \mathbb{R}^{nd}$ and $\boldsymbol{\beta}^{(b)} = (\boldsymbol{\beta}_1^{(b)T}, \dots, \boldsymbol{\beta}_{n_b}^{(b)T})^T \in \mathbb{R}^{n_b d}$, is convenient
 196 for the development. The constraint $\mathbf{C}_b \boldsymbol{\beta}^{(b)} = \mathbf{0} \in \mathbb{R}^{c_b d}$, where there are c_b constraints,
 197 combined with (4), (5), is now

$$\mathbf{Y} \mid \{\boldsymbol{\beta}^{(b)}\}_b, \mathbf{C}_b \boldsymbol{\beta}^{(b)} = \mathbf{0}, \boldsymbol{\Sigma}_\epsilon \sim \mathcal{N}_d \left(\sum_{b=0}^{B-1} \boldsymbol{\beta}^{(b)}, \mathbf{I}_n \otimes \boldsymbol{\Sigma}_\epsilon \right), \quad (8)$$

$$\boldsymbol{\beta}^{(b)} \mid \mathbf{C}_b \boldsymbol{\beta}^{(b)} = \mathbf{0}, \boldsymbol{\Sigma}_b \sim \mathcal{N}_{n_b d}(\mathbf{1}_{n_b} \otimes \boldsymbol{\beta}_0^{(b)}, \tilde{\boldsymbol{\Omega}}_b), \quad (9)$$

198 with \otimes denoting the Kronecker product. The rank-deficient $\tilde{\boldsymbol{\Omega}}_b$, due to the constraint,
 199 causes (9) to be improper. To derive this improper distribution begin with the uncon-
 200 strained and vectorized form of (5), which has covariance $\boldsymbol{\Omega}_b = \mathbf{I}_{n_b} \otimes \boldsymbol{\Sigma}_b$. The density is
 201 then stated through a decomposition of the precision, $\mathbf{Q}_b = \boldsymbol{\Gamma} \boldsymbol{\Lambda} \boldsymbol{\Gamma}^T \otimes \boldsymbol{\Sigma}_b^{-1}$. Assuming c_b
 202 constraints, the rank deficiency is introduced by removing the corresponding number of
 203 eigenvalues from the diagonal matrix $\boldsymbol{\Lambda}$, e.g. $\tilde{\boldsymbol{\Lambda}} = \text{diag}(0, \dots, 0, \lambda_{c_b+1}, \dots, \lambda_{n_b})$, leading to
 204 $\tilde{\mathbf{Q}}_b = \boldsymbol{\Gamma} \tilde{\boldsymbol{\Lambda}} \boldsymbol{\Gamma}^T \otimes \boldsymbol{\Sigma}_b^{-1}$. This method of addressing linear constraints is useful for other gen-
 205 eral improper distributions and intrinsic Gaussian Markov random fields, as illustrated
 206 by Rue and Held (2005). Let $|\mathbf{Q}|_*$ be the pseudo determinant of a singular matrix, that
 207 is, the product of its non-zero eigenvalues. In the case of the identity matrix being used
 208 as the first matrix term in the Kronecker product, the eigenvalues are one, thus densities
 209 of the likelihood, (8), and of batch level priors, (9) are

$$\begin{aligned} p(\mathbf{Y} \mid \{\boldsymbol{\beta}_j^{(b)}\}_b, \boldsymbol{\Sigma}_\epsilon) &\propto |\boldsymbol{\Sigma}_\epsilon|^{-n/2} \exp \left(-\frac{1}{2} \sum_{i=1}^n (\mathbf{Y}_i - \hat{\mathbf{Y}}_i)^T \boldsymbol{\Sigma}_\epsilon^{-1} (\mathbf{Y}_i - \hat{\mathbf{Y}}_i) \right. \\ &\quad \left. + -\frac{1}{2} \sum_{b=0}^{B-1} \sum_{j=1}^{n_b} (\boldsymbol{\beta}_j^{(b)} - \hat{\boldsymbol{\beta}}_j^{(b)})^T \frac{n}{n_b} \boldsymbol{\Sigma}_\epsilon^{-1} (\boldsymbol{\beta}_j^{(b)} - \hat{\boldsymbol{\beta}}_j^{(b)}) \right), \\ p(\boldsymbol{\beta}^{(b)} \mid \boldsymbol{\Sigma}_b) &\propto |\tilde{\mathbf{Q}}_b|_*^{1/2} \exp \left(-\frac{1}{2} (\boldsymbol{\beta}^{(b)} - \mathbf{1} \otimes \boldsymbol{\beta}_0^{(b)})^T \tilde{\mathbf{Q}}_b (\boldsymbol{\beta}^{(b)} - \mathbf{1} \otimes \boldsymbol{\beta}_0^{(b)}) \right) \\ &\propto |\boldsymbol{\Sigma}_b|^{-(n_b - c_b)/2} \exp \left(-\frac{1}{2} \sum_{j=c_b+1}^{n_b} (\boldsymbol{\beta}_j^{(b)} - \boldsymbol{\beta}_0^{(b)})^T \boldsymbol{\Sigma}_b^{-1} (\boldsymbol{\beta}_j^{(b)} - \boldsymbol{\beta}_0^{(b)}) \right), \end{aligned}$$

210 where $\hat{\cdot}$ denotes least-squares estimates. For orthogonal batches, the full posterior from
 211 these densities and from batch covariance prior densities, can be conveniently factored
 212 into

$$p(\boldsymbol{\Sigma}_\epsilon, \{\boldsymbol{\Sigma}_b, \boldsymbol{\beta}^{(b)}\}_{b=0}^{B-1} \mid \mathbf{Y}) = p(\boldsymbol{\Sigma}_\epsilon \mid \mathbf{Y}) \prod_{b=0}^{B-1} p(\boldsymbol{\Sigma}_b, \boldsymbol{\beta}^{(b)} \mid \mathbf{Y}, \boldsymbol{\Sigma}_\epsilon). \quad (10)$$

213 Each joint batch density, $p(\boldsymbol{\Sigma}_b, \boldsymbol{\beta}^{(b)} \mid \mathbf{Y}, \boldsymbol{\Sigma}_\epsilon)$, is then factored further. Using known matrix
 214 identities, e.g. $(\mathbf{A}^{-1} + \mathbf{B}^{-1})^{-1} = \mathbf{A}(\mathbf{A} + \mathbf{B})^{-1}\mathbf{B}$, the identity

$$\begin{aligned} & (\mathbf{x} - \mathbf{s})^T \mathbf{U}^{-1}(\mathbf{x} - \mathbf{s}) + (\mathbf{x} - \mathbf{t})^T \mathbf{V}^{-1}(\mathbf{x} - \mathbf{t}) \\ &= \text{tr} \left((\mathbf{U} + \mathbf{V})^{-1}(\mathbf{s} - \mathbf{t})(\mathbf{s} - \mathbf{t})^T \right) + (\mathbf{x} - \mathbf{P}^{-1}\mathbf{m})^T \mathbf{P}(\mathbf{x} - \mathbf{P}^{-1}\mathbf{m}), \end{aligned} \quad (11)$$

215 is derived, where $\mathbf{P} = \mathbf{U}^{-1} + \mathbf{V}^{-1}$, $\mathbf{m} = \mathbf{U}^{-1}\mathbf{s} + \mathbf{V}^{-1}\mathbf{t}$. Accounting for model constraints,
 216 together with (11), the batch superpopulation posterior and the batch levels are found
 217 through the decomposition of quadratic forms of batch levels and least squares estimates

$$\begin{aligned} & \text{tr} \left[\left(\boldsymbol{\Sigma}_\beta + \frac{n_b}{n} \boldsymbol{\Sigma}_\epsilon \right)^{-1} \mathbf{B}_b \right] + \sum_{j=1}^{c_b} (\boldsymbol{\beta}_j^{(b)} - \widehat{\boldsymbol{\beta}}_j^{(b)})^T \frac{n}{n_b} \boldsymbol{\Sigma}_\epsilon^{-1} (\boldsymbol{\beta}_j^{(b)} - \widehat{\boldsymbol{\beta}}_j^{(b)}) \\ &+ \sum_{j=c_b+1}^{n_b} (\boldsymbol{\beta}_j^{(b)} - \mathbf{P}_b^{-1}\mathbf{m}_j^{(b)})^T \mathbf{P}_b (\boldsymbol{\beta}_j^{(b)} - \mathbf{P}_b^{-1}\mathbf{m}_j^{(b)}), \end{aligned}$$

218 where $\mathbf{P}_b = \boldsymbol{\Sigma}_b^{-1} + \frac{n}{n_b} \boldsymbol{\Sigma}_\epsilon^{-1}$, $\mathbf{m}_j^{(b)} = \frac{n}{n_b} \boldsymbol{\Sigma}_\epsilon^{-1} \widehat{\boldsymbol{\beta}}_j^{(b)} + \boldsymbol{\Sigma}_b^{-1} \boldsymbol{\beta}_0^{(b)}$, and $\text{tr}(\cdot)$ denoting the trace
 219 operator. Additionally, $\mathbf{B}_b = \sum_{j=c_b+1}^{n_b} (\widehat{\boldsymbol{\beta}}_j^{(b)} - \boldsymbol{\beta}_0^{(b)})(\widehat{\boldsymbol{\beta}}_j^{(b)} - \boldsymbol{\beta}_0^{(b)})^T$, is analogous to a matrix
 220 sums of squares of the unconstrained batch level estimates that has been adjusted by the
 221 prior mean. The full joint posterior is then factored as

$$p(\boldsymbol{\Sigma}_\epsilon, \{\boldsymbol{\Sigma}_b, \boldsymbol{\beta}^{(b)}\}_{b=0}^{B-1} \mid \mathbf{Y}) = p(\boldsymbol{\Sigma}_\epsilon \mid \mathbf{Y}) \prod_{b=0}^{B-1} p(\boldsymbol{\Sigma}_b \mid \mathbf{Y}, \boldsymbol{\Sigma}_\epsilon) p(\boldsymbol{\beta}^{(b)} \mid \mathbf{Y}, \boldsymbol{\Sigma}_\epsilon, \boldsymbol{\Sigma}_b), \quad (12)$$

222 where the product denotes batch posterior independence, and thus no need for computa-
 223 tionally intensive MCMC procedures. The corresponding distributions of (12) are

$$\boldsymbol{\Sigma}_\epsilon \mid \mathbf{Y} \sim W^{-1} \left(\boldsymbol{\Psi}_\epsilon + \sum_{i=1}^n (\mathbf{Y}_i - \widehat{\mathbf{Y}}_i)(\mathbf{Y}_i - \widehat{\mathbf{Y}}_i)^T, \kappa_\epsilon + n - \sum_{b=0}^{B-1} n_b \right), \quad (13)$$

$$\boldsymbol{\Sigma}_b + \frac{n_b}{n} \boldsymbol{\Sigma}_\epsilon \mid \mathbf{Y}, \boldsymbol{\Sigma}_\epsilon \sim W^{-1} (\boldsymbol{\Psi}_b + \mathbf{B}_b, \kappa_b + n_b - c_b), \quad (14)$$

$$\boldsymbol{\beta}_j^{(b)} \mid \mathbf{Y}, \boldsymbol{\Sigma}_\epsilon, \boldsymbol{\Sigma}_b \sim \begin{cases} \mathcal{N}_d \left(\widehat{\boldsymbol{\beta}}_j^{(b)}, \frac{n_b}{n} \boldsymbol{\Sigma}_\epsilon \right) & j = 1, \dots, c_b, \\ \mathcal{N}_d \left(\mathbf{P}_b^{-1} \mathbf{m}_j^{(b)}, \mathbf{P}_b^{-1} \right) & j = c_b + 1, \dots, n_b. \end{cases} \quad (15)$$

224 Batch levels (15), which reflect both free and constrained parameter estimates, can then
 225 be sampled and adjusted accordingly to obtain posteriors for finite-population covari-
 226 ances, \mathbf{S}_b . Recall finite-population parameters focus on observed levels of a batch, not on
 227 all potential unobserved batch levels.

228 2.2.3 Covariance Posteriors

229 In all cases thus far covariances Σ_b are assumed to be of full rank. Hence, improper
230 covariance posteriors will be due only to an insufficient number of observed levels of the
231 batch. Díaz-García *et al.* (1997) offer a comprehensive look at all possible cases of im-
232 proper Wishart distributions and following their terminology this would be classified as
233 a pseudo-inverse-Wishart. Uhlig (1994) as well as Srivastava (2003) consider sampling
234 with a pseudo-singular-Wishart distribution. Extending their work to inverse-Wishart
235 distributions is one method for dealing with moderate discrepancies in the number of
236 observed levels, $n_b < d$. Addressing cases in which $n_b \ll d$ is discussed in Section 4. Even
237 in the remaining case, $n_b \geq d$, simulation from a posterior is not always efficient. Because
238 support of the inverse-Wishart posterior requires positive definiteness in two respects,
239 $\Sigma_\beta > 0$, and $\Sigma_\beta - \frac{n_b}{n}\Sigma_\epsilon > 0$, the usual method of rejection sampling from an inverse-
240 Wishart distribution is not always practical. Everson and Morris (2000) describe a more
241 computationally efficient method to maintain positive definiteness through a Cholesky
242 decomposition and maintaining positive eigenvalues while the sample realization is gen-
243 erated.

244 2.2.4 Analysis Results

245 Multivariate sources of variability do not always yield a single, clear criterion that in-
246 dicates the greatest contributor to overall variability. For scalar variance components,
247 $\sigma_b^2 > \sigma_\epsilon^2$ is clearly interpreted, however, due to the partial ordering of positive definite
248 matrices, the analogous statement on covariance matrices is not useful. In other words,
249 there is not a single, obvious comparison that can be made to determine which of two
250 covariances are “greater”. Depending on the setting, there may exist an adequate scalar
251 that sufficiently summarizes covariance characteristics. For the volume of ellipsoidal con-
252 tours the determinant, $|\Sigma|$, achieves this, while in other cases the sum of all entries,
253 $\mathbf{1}^T \Sigma \mathbf{1}$, or the sum of the marginal variances, $\text{tr}(\Sigma)$, may be appropriate. Scalar criteria
254 with corresponding uncertainty intervals then allow multivariate sources of variability to

255 be directly compared. Mardia *et al.* (1979) employed the determinant and trace, which
 256 correspond to the product and sum of eigenvalues; referring to them as the generalized
 257 variance and total variance, respectively. We have amended the terminology, since inclu-
 258 sion of the sum of all matrix elements requires further delineation, by denoting $\mathbf{1}^T \boldsymbol{\Sigma} \mathbf{1}$ as
 259 the total variance, and $\text{tr}(\boldsymbol{\Sigma})$ as the total marginal variance.

260 Effectively relaying results of analysis of variance is one of the motivating factors
 261 that Gelman (2005) cites. The classical table of p -values does not yield any indication
 262 of batches with the largest variances, nor are the required assumptions on other batches
 263 clear. Nelder (1999) discusses many of the issues of over-reliance upon the p -value, and its
 264 ineffectiveness as a tool for communicating results. Uncertainty intervals are the default
 265 choice for presenting results. Visual plots are convenient since they facilitate simultaneous
 266 comparison of the relative variability contributions, their magnitudes, and the magnitude
 267 of the uncertainty in the estimates. For direct comparison of batches b and b' , statements
 268 of the form $P(g(\boldsymbol{\Sigma}_b) > g(\boldsymbol{\Sigma}_{b'}) \mid \mathbf{Y})$, utilizing an arbitrary matrix criterion $g(\cdot)$, may also
 269 be found.

270 3 Examples

271 This section covers two examples of the outlined methodology to carry out confirmatory
 272 procedures on multivariate data. The first is a toy example in which output and sum-
 273 maries are given in order to provide further insight. The second example utilizes global
 274 averages of temperature and precipitation predictions using 13 atmosphere-ocean gen-
 275 eral circulation models and 3 global greenhouse gas emissions scenarios that have been
 276 identified by the Intergovernmental Panel on Climate Change.

277 3.1 Simulation

278 The process $\mathbf{Y}_{ij} = \boldsymbol{\mu} + \boldsymbol{\alpha}_i + \boldsymbol{\epsilon}_{ij} \in \mathbb{R}^d$, i.e. $B = 2$, $d = 3$, is used to illustrate the method
 279 of Section 2.2. To generate the three-dimensional observations, parameters $\boldsymbol{\Sigma}_\alpha$, $\boldsymbol{\Sigma}_\epsilon$, and
 280 $\boldsymbol{\mu}$ are fixed. An individual simulation is then performed by generating $\boldsymbol{\alpha}_i$ and $\boldsymbol{\epsilon}_{ij}$, $i =$

281 $1, \dots, n_\alpha$, $j = 1, \dots, n_\epsilon$, from mean-zero multivariate Gaussian distributions with their
 282 respective fixed covariances. The mean term $\boldsymbol{\mu}$ is added to generated data resulting in
 283 $n = n_\alpha n_\epsilon$ observations.

284 Using (13)–(15), posterior distributions for these covariance criteria are obtained for
 285 three distinct simulation scenarios. The three scenarios can be explained by the am-
 286 biguous description that variability introduced by batch $\boldsymbol{\alpha}$ is greater than (case 1), less
 287 than (case 2), or comparable to (case 3) variability introduced by error batch $\boldsymbol{\epsilon}$. More
 288 specifically, covariance matrices are decomposed into a vector of marginal standard devi-
 289 ations \boldsymbol{s} and a correlation matrix \mathbf{R} , e.g. $\boldsymbol{\Sigma}_\alpha = \text{diag}(\boldsymbol{s}_\alpha)\mathbf{R}_\alpha\text{diag}(\boldsymbol{s}_\alpha)$. For all simulation
 290 correlation matrices are fixed. Batch levels $\boldsymbol{\alpha}_i$ have the unique correlation structure
 291 $(\mathbf{R}_\alpha)_{1,2} = 0.3$, $(\mathbf{R}_\alpha)_{1,3} = 0.1$, $(\mathbf{R}_\alpha)_{2,3} = 0.5$. Errors $\boldsymbol{\epsilon}_{ij}$ have the correlation matrix, \mathbf{R}_ϵ ,
 292 with autocorrelation structure $(\mathbf{R}_\epsilon)_{i,j} = \rho^{|i-j|}$, and $\rho = 0.2$. Error marginal variances are
 293 additionally held constant at 1 over all simulations, $\boldsymbol{\Sigma}_\epsilon = \mathbf{R}_\epsilon$, so that only \boldsymbol{s}_α is distinct
 294 for each case.

295 The objective of the analysis is to assess the relative variability introduced by batch
 296 $\boldsymbol{\alpha}$ and batch $\boldsymbol{\epsilon}$, as well as the uncertainty in the assessment. Further, this is to be done in
 297 an appropriate multivariate context. Figure 1 displays the results of two simulation runs
 298 under the first scenario (case 1) using the determinant. In one simulation, the number
 299 of batch level realizations are $n_\alpha = 5$, $n_\epsilon = 3$ and in the second $n_\alpha = 8$, $n_\epsilon = 5$, which is
 300 to say less vs. more data. The left-most graph of Figure 1 displays uncertainty intervals,
 301 with narrow lines denoting 95% quantiles, thicker lines 50%, and a vertical tick placed
 302 at the median. The upper set of intervals, which are intuitively wider, correspond to less
 303 data, while the lower set of intervals correspond to more. By vertical comparison of the
 304 uncertainty intervals, we see that for $n_\alpha = 5$, $n_\epsilon = 3$ all intervals overlap, and hence no
 305 distinction can be made between the sources of variability. For $n_\alpha = 8$, $n_\epsilon = 5$ however,
 306 there is no overlap of the uncertainty intervals, suggesting that both superpopulation
 307 variability, and the finite-population variability are greater than error variability. Ad-
 308 ditionally, Figure 1 offers a diagnostic look at covariance posteriors. The center figure

309 displays ellipses from first two principal components corresponding to 2.5%, 50%, and
 310 97.5% determinant-ordered percentiles of the posterior distributions, specific values of
 311 which can be seen on endpoints of the uncertainty intervals. The right-most graph of
 312 Figure 1, which shows all 1000 ellipses from each posterior distribution, offers a look at
 313 the size, shape, and orientation, for an overall comparison of the uncertainty in the batch
 314 covariances. Size renders an idea of the magnitude of the marginal variances. The dis-
 315 parity in size between the ellipses corresponding to \mathbf{S}_α and $\mathbf{\Sigma}_\epsilon$ suggest that the marginal
 316 variances of the former are greater than those of the latter. Through shape, one may
 317 glean some insight into batch covariance dependence. Lastly, the orientation, or varying
 318 orientation, suggests the uncertainty of the dependence, e.g. as the orientation of the
 319 ellipses corresponding to $\mathbf{\Sigma}_\alpha$ fluctuate greatly, there is not much that can be said about
 320 its dependence structure.

321 For comparison, consider a frequentist approach to a simplified form of the problem.
 322 Beginning with $\mathbf{X}_i \sim \mathcal{N}_d(\mathbf{0}, \mathbf{\Sigma})$, $i = 1, \dots, n$, it is known that $\mathbf{U} = \sum_i (\mathbf{X}_i - \bar{\mathbf{X}})(\mathbf{X}_i - \bar{\mathbf{X}})^T \sim$
 323 $W_d(\mathbf{\Sigma}, n - 1)$, from which we derive the distributions

$$\begin{aligned}
 |\mathbf{U}| &\sim |\mathbf{\Sigma}| \cdot \prod_{i=1}^d \chi_{n-1-d+i}^2, \\
 \mathbf{1}^T \mathbf{U} \mathbf{1} &\sim \mathbf{1}^T \mathbf{\Sigma} \mathbf{1} \cdot \chi_{n-1}^2, \\
 \text{tr}(\mathbf{U}) &\sim \sum_{i=1}^d \lambda_i \cdot \chi_{n-1}^2, \quad \lambda_1, \dots, \lambda_d = \text{eig}(\mathbf{\Sigma}).
 \end{aligned}$$

324 The first two offer pivots and thus allow for closed form expressions that yield confidence
 325 intervals for values of interest $|\mathbf{\Sigma}|, \mathbf{1}^T \mathbf{\Sigma} \mathbf{1}$. The confidence interval for $\text{tr}(\mathbf{\Sigma})$ is based on
 326 the normal approximation that matches the first two moments, $E\{\text{tr}(\mathbf{U})\} = (n - 1)\text{tr}(\mathbf{\Sigma})$,
 327 and $\text{Var}\{\text{tr}(\mathbf{U})\} = 2(n - 1)\text{tr}(\mathbf{\Sigma}^2)$. This approximation has been chosen in the spirit of
 328 moment matching approximations used by Imhof (1961) as applied to quadratic forms
 329 of random vectors. Note that these confidence intervals assume that the α_i are directly
 330 observed, which is not the case for our proposed method. Rather, the classical methods
 331 shown are included only for comparison.

332 To gain insight into the coverage success and uncertainty interval widths, we have

333 carried out $S = 100$ simulations over different values of n_α and each of the different
 334 scenarios of variability sources. For all simulations the number of replicates at each level
 335 is fixed at $n_\epsilon = 15$. Results in all 3 cases were relatively similar with respect to coverage,
 336 noting however that uncertainty interval widths increase as the magnitude of variability
 337 increases. Thus, only the scenario in which variability sources are comparable (case 3)
 338 has been shown (Figure 2). Coverage and interval widths for Σ_α and Σ_{Freq} should be
 339 compared as they correspond to the same true, unknown covariance. Despite the fact
 340 that the methodology does not assume realizations of α to be observed directly, but
 341 rather indirectly through \mathbf{Y} , results are comparable to the frequentist approach outlined.

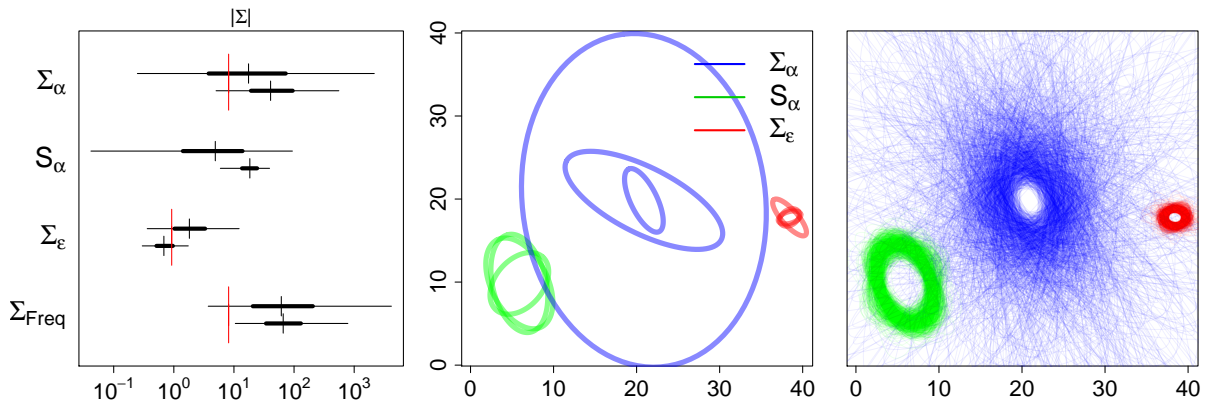


Figure 1: Simulation for two distinct sample size pairs, $n_\alpha = 5, n_\epsilon = 3$, and $n_\alpha = 8, n_\epsilon = 5$. In both, batch α varies greater than the errors, with $\mathbf{s}_\alpha = (\sqrt{2}, \sqrt{2}, \sqrt{3})^T$. Uncertainty intervals with thin narrow lines denoting 95% uncertainty level endpoints, thicker middle portion denoting 50% endpoints, and vertical tick at median. Larger red vertical ticks denote true parameter values. Higher-positioned, wider intervals correspond to smaller batch sample sizes, while lower-positioned, narrower intervals correspond to larger batch sample sizes (left). For second set of sample size pairs, ellipses from first two principal components are displayed for 2.5%, 50%, and 97.5% determinant-ordered percentiles of posterior distributions when 1000 posterior realizations have been drawn (center). All 1000 posterior ellipses (right).

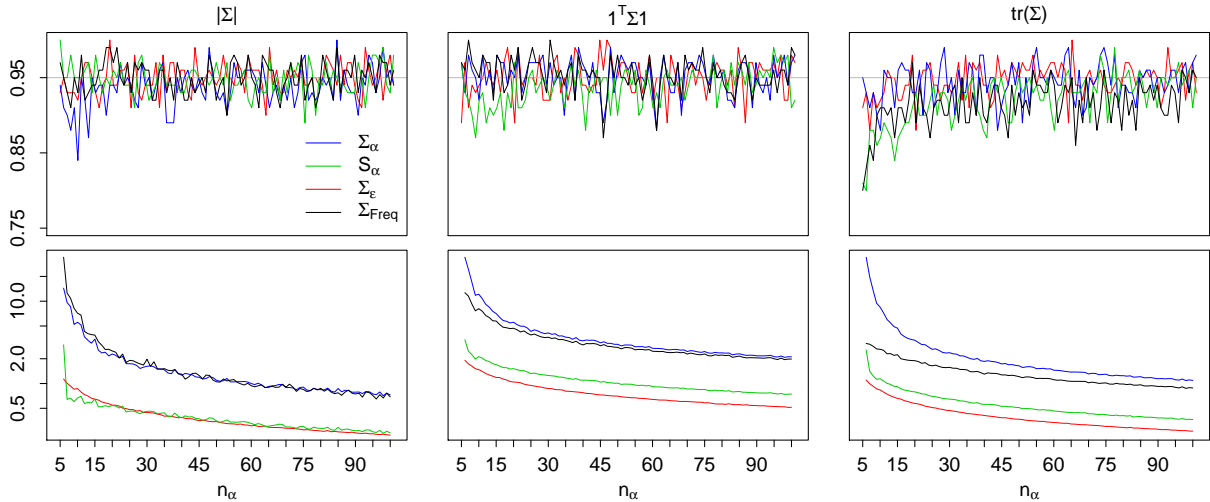


Figure 2: For $n_\alpha = 5, \dots, 100$, coverage is estimated with $S = 100$ simulations in which the sources of variability are comparable (case 3). Coverage estimates for Σ_α , \mathbf{S}_α , and Σ_ϵ , where grey line denotes 95% nominal coverage (top). Average uncertainty interval widths on log scale (bottom).

3.2 Application

In this example our methodology is applied to a bivariate dataset of global temperature (Celsius) and precipitation (mm/day) for 9 decadal averages of boreal summer months, June, July, August, during the remaining century. The first batch in the model consists of 13 levels, each representing a single atmosphere-ocean general circulation model (AOGCM) developed by several international climate research institutions as part of the CMIP3 project (Meehl *et al.*, 2000) in the framework of the Fourth Assessment Report (AR4) for the Intergovernmental Panel on Climate Change (IPCC). The second batch covers 3 greenhouse gas emissions scenarios that have been defined by the Special Report on Emissions Scenarios (SRES), which are identified as A1B, A2, and B1 (Nakićenović and Swart, 2000). One fundamental objective of the analysis is then to compare how these factors contribute to overall variability of global climate averages, how they relate to one another, and what the uncertainty of this assessment is.

Bias and dependence among climate models is an issue that has more recently begun to be examined further, beginning with Tebaldi and Knutti (2007), Jun *et al.* (2008), Knutti *et al.* (2010), and references therein. Despite this, we adopt the statistical assumption

358 that has traditionally been used when working with sets of AOGCMs, which is
 359 to assume that they are independently drawn from a common process representative of
 360 true climate characteristics. Using this assumption our approach can be seen as a useful
 361 exploratory tool, and may be further adopted to address contrasts of batch levels, and
 362 thus to identify similar batch levels. Preliminary analysis steps have suggested the model

$$\mathbf{Y}_{ijt} = \boldsymbol{\mu}_0 + \boldsymbol{\alpha}_{0,i} + \boldsymbol{\beta}_{0,j} + \boldsymbol{\gamma}_{ij} + x_{1,t}\boldsymbol{\mu}_1 + x_{1,t}\boldsymbol{\alpha}_{1,i} + x_{1,t}\boldsymbol{\beta}_{1,j} + x_{2,t}\boldsymbol{\mu}_2 + \boldsymbol{\epsilon}_{ijt}, \quad (16)$$

363 where $i = 1, \dots, n_\alpha = 13$, $j = 1, \dots, n_\beta = 3$, $t = 1, \dots, n_t = 9$, $n = n_\alpha n_\beta n_t$, and $d = 2$.
 364 Time covariate x_1 is centered such that $x_{1,t} = -4, \dots, 4$, and x_2 is transformed to be
 365 orthogonal to other predictors in the model. Batches of interest are AOGCM, $\boldsymbol{\alpha}$, and
 366 SRES, $\boldsymbol{\beta}$, and their interaction, $\boldsymbol{\gamma}$. The first two are further specified as a constant effect,
 367 $\boldsymbol{\alpha}_0, \boldsymbol{\beta}_0$, as well as with respect to time, $\boldsymbol{\alpha}_1, \boldsymbol{\beta}_1$.

368 Posterior distributions of batches $\boldsymbol{\alpha}_0, \boldsymbol{\beta}_0$, and $\boldsymbol{\gamma}$ are derived from (14) and (15).
 369 Batches $\boldsymbol{\alpha}_1$ and $\boldsymbol{\beta}_1$ differ slightly as they correspond to the regression model formulation.
 370 Multivariate batch levels associated with a covariate would, in general, be multiplied by
 371 a matrix, e.g. $\mathbf{X}_{1,t}$. Using a matrix covariate, superpopulation and batch level posteriors
 372 of batch $\boldsymbol{\alpha}_1$ are then

$$\boldsymbol{\Sigma}_{\alpha_1} + \mathbf{V}_{\alpha_1} \mid \mathbf{Y}, \boldsymbol{\Sigma}_\epsilon \sim W^{-1} \left(\sum_{i=c_{\alpha_1}+1}^{n_\alpha} \hat{\boldsymbol{\alpha}}_{1,i} \hat{\boldsymbol{\alpha}}_{1,i}^T, n_\alpha - c_{\alpha_1} \right), \quad (17)$$

$$\boldsymbol{\alpha}_{1,i} \mid \mathbf{Y}, \boldsymbol{\Sigma}_\epsilon, \boldsymbol{\Sigma}_{\alpha_1} \sim \begin{cases} \mathcal{N}_d(\hat{\boldsymbol{\alpha}}_{1,i}, \frac{n_b}{n} \boldsymbol{\Sigma}_\epsilon) & i = 1, \dots, c_{\alpha_1}, \\ \mathcal{N}_d(\mathbf{P}_{\alpha_1}^{-1} \mathbf{m}_{\alpha_1,i}, \mathbf{P}_{\alpha_1}^{-1}) & i = c_{\alpha_1} + 1, \dots, n_\alpha, \end{cases} \quad (18)$$

373 where $\mathbf{V}_{\alpha_1} = \frac{1}{n_\beta} (\sum_{t=1}^{n_t} \mathbf{X}_{1,t}^T \boldsymbol{\Sigma}_\epsilon^{-1} \mathbf{X}_{1,t})^{-1}$, $\mathbf{P}_{\alpha_1} = \boldsymbol{\Sigma}_{\alpha_1}^{-1} + \mathbf{V}_{\alpha_1}^{-1}$, and $\mathbf{m}_{\alpha_1,i} = \mathbf{V}_{\alpha_1}^{-1} \hat{\boldsymbol{\alpha}}_{1,i}$. For
 374 model (16) the covariate matrix is $\mathbf{X}_{1,t} = \text{diag}(x_{1,t})$, and thus $\mathbf{V}_{\alpha_1} = (n_\beta \sum_{t=1}^{n_t} x_{1,t}^2)^{-1} \boldsymbol{\Sigma}_\epsilon$.
 375 The posterior of batch $\boldsymbol{\beta}_1$ is found similarly.

376 Figure 3 suggests that AOGCM is the most distinguishing feature. Figures 4 and
 377 5 confirm this assessment since $\boldsymbol{\alpha}_0$ is seen as the most significant source of variability
 378 among all batches. Comparison of Figures 4, 5 also illustrate the additional uncertainty
 379 of superpopulation parameters over their finite-population counterparts. Superpopulation

380 covariance criteria uncertainty intervals are wide because they account for uncertainty
 381 in unobserved batch levels, particularly in the case when a small number of batch lev-
 382 els have been observed. Finite-population covariance uncertainty intervals are generally
 383 smaller, because they are concerned with variability of only the batch levels that have
 384 been realized.

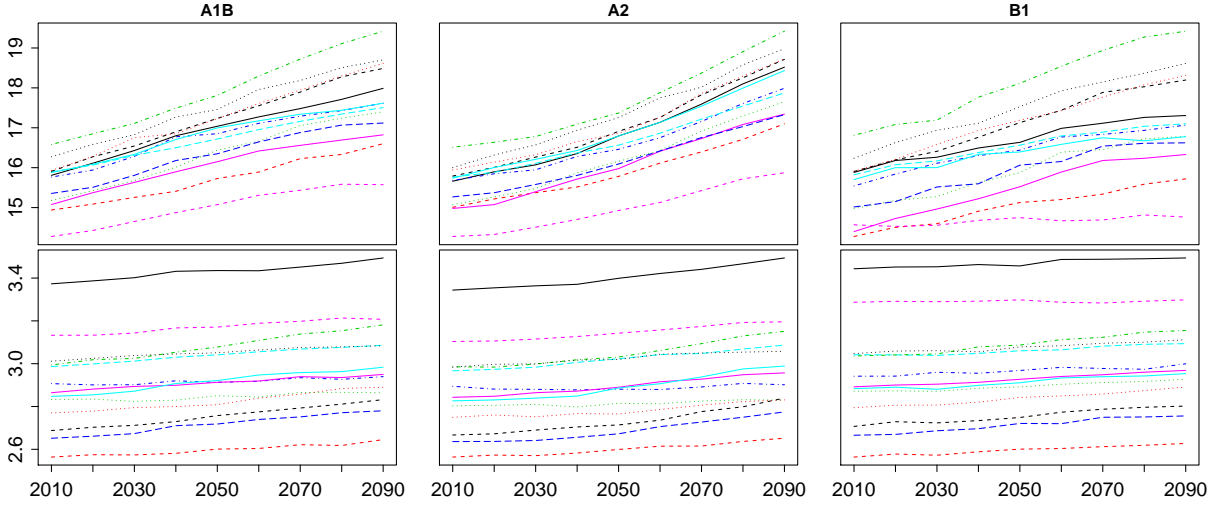


Figure 3: Global temperature (top) in degrees Celsius and precipitation (bottom) as mm/day over $n_t = 9$ decadal intervals for $n_\alpha = 13$ AOGCMs and $n_\beta = 3$ emissions scenarios.

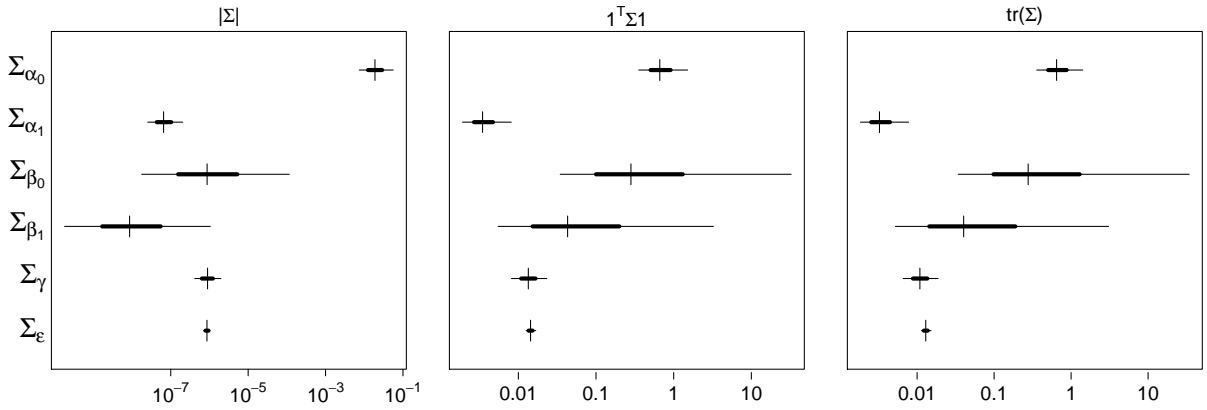


Figure 4: Superpopulation covariance uncertainty intervals using determinant, total variance, and total marginal variance criteria shown on a log scale. Nominal coverages of 0.95 (thin lines) and 0.50 (thick lines), and the median (vertical line) are denoted using quantiles of the corresponding posterior distributions.

385 Posterior predictive distributions, often used to perform model checking and diagnos-

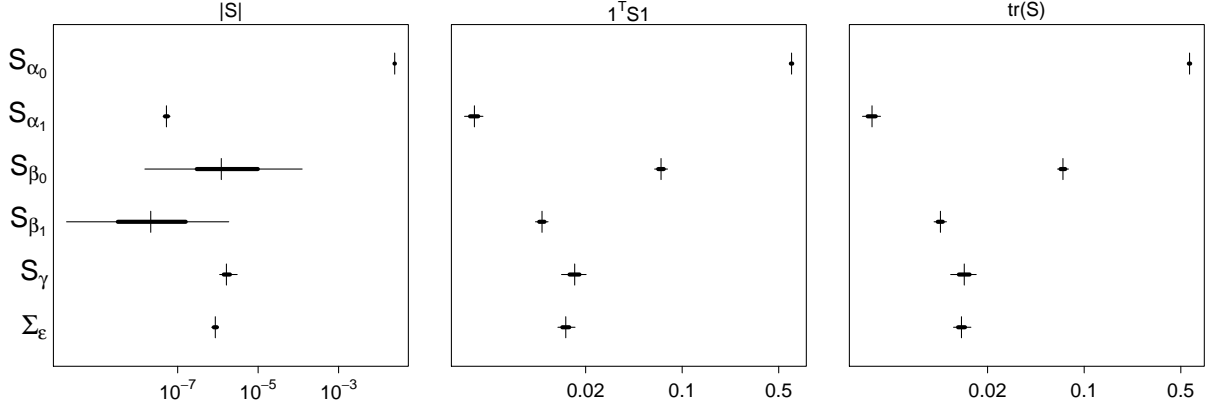


Figure 5: Finite-population covariance uncertainty intervals using determinant, total variance, and total marginal variance criteria shown on a log scale. Nominal coverages of 0.95 (thin lines) and 0.50 (thick lines), and the median (vertical line) are denoted using quantiles of the corresponding posterior distributions.

386 tics, can also be utilized to identify distinct sources of variability. The posterior predictive
387 is conditional on observations with levels from each batch assumed to be, a) the same as
388 those batch levels that have been observed data, b) unobserved/novel batch level realiza-
389 tions. Figure 6 examines posterior density $p(\tilde{\mathbf{Y}}_{ijn_t} - \tilde{\mathbf{Y}}_{ij1} | \{\mathbf{Y}_{ijt}\})$, the difference between
390 posterior predictive distributions at the final, $t = n_t$, and initial, $t = 1$, decades. Thus,
391 the focus is on temporal batches, $\boldsymbol{\alpha}_{1i'}$, $\boldsymbol{\beta}_{1j'}$. Indices i', j' signify new, unobserved batch
392 levels. Linear and quadratic terms, $\boldsymbol{\mu}_1, \boldsymbol{\mu}_2$ are included, although additional variability
393 from these terms has been disregarded. The left-most panel, in which every batch con-
394 tributes a new batch level realization, shows a large degree of variation. The center panel
395 assumes that the AOGCM observed in the original data is to be used, thus variability
396 from these specific batch level posteriors is included. For SRES a novel batch level is
397 assumed, thus a realization utilizing the SRES superpopulation posteriors is included.
398 A subset of three observed AOGCM levels has been displayed, selected so as to best
399 represent the range and relative distances of their peaks. However, the high degree of
400 variation introduced by the new emissions scenario level makes even these distributions
401 nearly indistinguishable. In the right-most plot, using observed emissions batch levels,
402 $n_\beta = 3$, the additional variability introduced comes primarily from the new AOGCM

403 batch level to be observed. The posterior predictive plots are particularly useful for de-
 404 termining whether the variability from each batch is due to the magnitude of the batch
 405 variability itself, or due to uncertainty in the assessment itself.

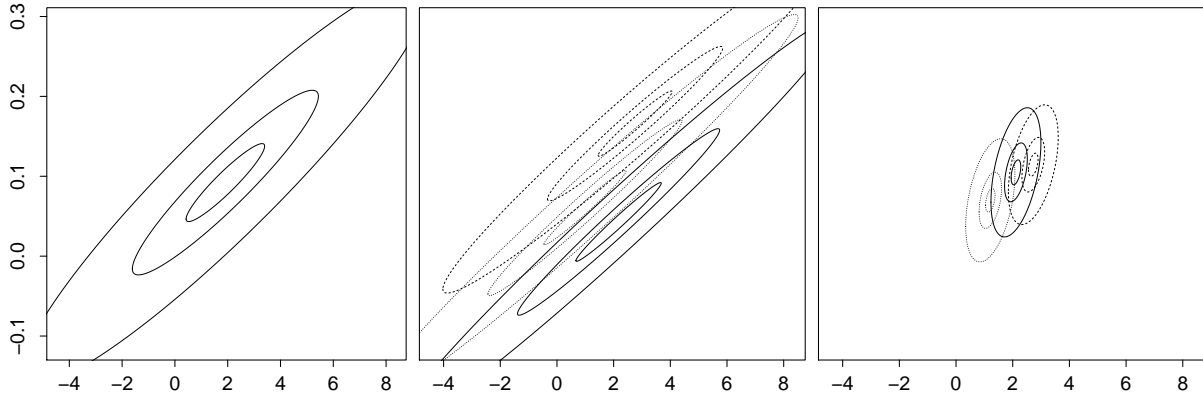


Figure 6: Posterior predictive distribution, $p(\mathbf{Y}_{i'j'n_t} - \mathbf{Y}_{i'j'1} | \{\mathbf{Y}_{ijt}\})$, where both i', j' represent new, unobserved AOGCM and SRES batch levels (left). Posterior predictive $p(\mathbf{Y}_{ij'n_t} - \mathbf{Y}_{ij'1} | \{\mathbf{Y}_{ijt}\})$ with observed AOGCM batch levels, $i = 3, 9, 12$ (solid, dashed, dotted) and unobserved SRES batch level $\beta_{1,j'}$ (center). Posterior predictive $p(\mathbf{Y}_{i'jn_t} - \mathbf{Y}_{i'j1} | \{\mathbf{Y}_{ijt}\})$ with unobserved AOGCM batch level $\alpha_{1,i'}$ and all SRES levels, $j = 1, 2, 3$ (solid, dashed, dotted), that have been observed (right). Density contours correspond to quantiles 0.05, 0.25, 0.75. Horizontal and vertical axes denote precipitation in mm/day and temperature in degrees Celsius, respectively.

406 4 Discussion

407 The first contribution of this paper has been in extending recent philosophical shifts in
 408 the treatment of analysis of variance to multivariate settings. New analysis of variance
 409 approaches allow appropriate parameters, e.g. super or finite population, to be used to
 410 answer the correct research question, while at the same time providing coherent model
 411 definition, implementation, and interpretation. This same flexibility has been extended
 412 to multivariate cases; in that the researcher can guide covariance criteria choices, rather
 413 than the method determining the criterion. The second contribution has been in provid-
 414 ing a foundation for computational efficiency, which is necessary for dimension scalability.

415 Using improper batch level priors we have shown that it is possible to minimize depen-
416 dencies between batch covariances. In many cases this reduces, or eliminates, the need
417 for complex and computationally demanding analyses.

418 Further extensions to the methodology must explicitly address increasing dimension-
419 ality. For moderately sized dimensions d , relative to number of observations, improper
420 inverse-Wishart distributions, and/or priors that impose particular dependence struc-
421 tures, are possible options. For cases in which d is very large, stricter covariance as-
422 sumptions may be employed. In the spatial context, properties such as stationarity allow
423 covariance parameter space to be reduced, e.g. range, sill, and nugget in a spatial covari-
424 ance function. Because simultaneous estimation of such parameters is nontrivial, some
425 parameters are often assumed, or estimated empirically in earlier analysis steps, as in
426 Furrer *et al.* (2007). In other cases, so as to maintain computational feasibility, spar-
427 sity restrictions are placed on covariances (Cressie and Johannesson, 2008; Furrer *et al.*,
428 2006; Stein, 2008). For many such scenarios a covariance is decomposed into a correla-
429 tion matrix and a scalar variance parameter. Our method is then carried out with the
430 inverse-Wishart posterior density transformed through a spectral decomposition of the
431 correlation matrix, thus allowing for efficient posterior sampling for cases in which $d \gg n$.
432 This extension offers an alternative to geostatistical model analyses that have previously
433 relied on computationally intensive MCMC methods, and is the focus of current research.
434 Other difficulties encountered are unbalanced designs and linearly dependent predictors.
435 MCMC may be utilized for sets of dependent batch levels. Development for these cases
436 is another area of current research.

437 **Acknowledgments**

438 We acknowledge the modeling groups, the Program for Climate Model Diagnosis and In-
439 tercomparison (PCMDI) and the WCRP's Working Group on Coupled Modeling (WGCM)
440 for their roles in making available the WCRP CMIP3 multi-model dataset. Support of
441 this dataset is provided by the Office of Science, U.S. Department of Energy.

442 References

- 443 Cressie, N. and Johannesson, G. (2008). Fixed rank kriging for very large spatial data
444 sets. *J. R. Stat. Soc. Ser. B Stat. Methodol.*, **70**, 209–226.
- 445 Daniels, M. J. (1999). A prior for the variance in hierarchical models. *Canad. J. Statist.*,
446 **27**, 567–578.
- 447 Daniels, M. J. and Kass, R. E. (2001). Shrinkage estimators for covariance matrices.
448 *Biometrics*, **57**, 1173–1184.
- 449 Díaz-García, J. A., Gutierrez Jáimez, R., and Mardia, K. V. (1997). Wishart and pseudo-
450 Wishart distributions and some applications to shape theory. *J. Multivariate Anal.*,
451 **63**, 73–87.
- 452 Everson, P. J. and Morris, C. N. (2000). Simulation from Wishart distributions with
453 eigenvalue constraints. *J. Comput. Graph. Statist.*, **9**, 380–389.
- 454 Furrer, R., Genton, M. G., and Nychka, D. (2006). Covariance tapering for interpolation
455 of large spatial datasets. *J. Comput. Graph. Statist.*, **15**, 502–523.
- 456 Furrer, R., Sain, S. R., Nychka, D. W., and Meehl, G. A. (2007). Multivariate Bayesian
457 analysis of atmosphere-ocean general circulation models. *Environ. Ecol. Stat.*, **14**,
458 249–266.
- 459 Gelman, A. (2005). Analysis of variance: Why it is more important than ever. *Ann.*
460 *Statist.*, **33**, 1–31.
- 461 Gelman, A. and Hill, J. (2006). *Data Analysis Using Regression and Multi-*
462 *level/Hierarchical Models*. Cambridge University Press, 1st edition.
- 463 Imhof, J. P. (1961). Computing the distribution of quadratic forms in normal variables.
464 *Biometrika*, **48**, 419–426.

465 Jun, M., Knutti, R., and Nychka, D. W. (2008). Spatial analysis to quantify numerical
466 model bias and dependence: How many climate models are there? *J. Amer. Statist.*
467 *Assoc.*, **103**, 934–947.

468 Kaufman, C. G. and Sain, S. R. (2010). Bayesian functional ANOVA modeling using
469 Gaussian process prior distributions. *Bayesian Anal.*, **5**, 847–874.

470 Knutti, R., Furrer, R., Tebaldi, C., Cermak, J., and Meehl, G. A. (2010). Challenges in
471 combining projections from multiple climate models. *Journal of Climate*, **23**, 2739–
472 2758.

473 Leinonen, T., O’Hara, R. B., Cano, J. M., and Merilä, J. (2008). Comparative stud-
474 ies of quantitative trait and neutral marker divergence: a meta-analysis. *Journal of*
475 *Evolutionary Biology*, **21**, 1–17.

476 Lencina, V. B., Singer, J. M., and Stanek, E. J. (2005). Much ado about nothing: the
477 mixed models controversy revisited. *International Statistical Review*, **73**, 9–20.

478 Lindgren, F., Rue, H., and Lindström, J. (2011). An explicit link between gaussian
479 fields and gaussian markov random fields: the stochastic partial differential equation
480 approach. *J. R. Stat. Soc. Ser. B Stat. Methodol.*, **73**, 423–498.

481 Mardia, K. V., Kent, J. T., and Bibby, J. M. (1979). *Multivariate Analysis*. Academic
482 Press.

483 Meehl, G. A., Boer, G. J., Covey, C., Latif, M., and Stouffer, R. J. (2000). The coupled
484 model intercomparison project (CMIP). *American Meteorological Society Bulletin*, **81**,
485 313–318.

486 Nakićenović, N. and Swart, R., editors (2000). *Special Report on Emission Scenarios*.
487 Intergovernmental Panel on Climate Change, Cambridge University Press.

488 Nelder, J. A. (1977). A reformulation of linear models. *J. Roy. Statist. Soc. Ser. A*, **140**,
489 48–77.

- 490 Nelder, J. A. (1994). The statistics of linear models: back to basics. *Statist. Comput.*, **4**,
491 221–234.
- 492 Nelder, J. A. (1999). From statistics to statistical science. *J. R. Stat. Soc. Ser. D The*
493 *Statistician*, **48**, 257–269.
- 494 Nelder, J. A. (2008). What is the mixed-models controversy? *International Statistical*
495 *Review*, **76**, 134–135.
- 496 Qian, S. S. and Shen, Z. (2007). Ecological applications of multilevel analysis of variance.
497 *Ecology*, **88**, 2489–2495.
- 498 Rue, H. and Held, L. (2005). *Gaussian Markov Random Fields: Theory and Applications*.
499 Chapman & Hall, London.
- 500 Rue, H., Martino, S., and Chopin, N. (2009). Approximate Bayesian inference for latent
501 gaussian models by using integrated nested laplace approximations. *J. R. Stat. Soc.*
502 *Ser. B Stat. Methodol.*, **71**, 1–35.
- 503 Sain, S. R., Nychka, D., and Mearns, L. (2011). Functional ANOVA and regional climate
504 experiments: a statistical analysis of dynamic downscaling. *Environmetrics*, **22**, 700–
505 711.
- 506 Srivastava, M. S. (2003). Singular Wishart and multivariate beta distributions. *Ann.*
507 *Statist.*, **31**, 1537–1560.
- 508 Stein, M. L. (2008). A modeling approach for large spatial datasets. *J. Korean Statist.*
509 *Soc.*, **37**, 3–10.
- 510 Tebaldi, C. and Knutti, R. (2007). The use of the multi-model ensemble in probabilistic
511 climate projections. *Philos. Trans. R. Soc. Lond. Ser. A Math. Phys. Eng. Sci.*, **365**,
512 2053–2075.
- 513 Uhlig, H. (1994). On singular Wishart and singular multivariate beta distributions. *Ann.*
514 *Statist.*, **22**, 395–405.

515 Voss, D. T. (1999). Resolving the mixed models controversy. *Amer. Statist.*, **53**, 352–356.